9. T. Bachels, R. Schafer, H. J. Guntherodt, *Phys. Rev. Lett.* **84**, 4890 (2000).
10. L. Q. Yang, A. E. DePristo, *J. Catal.* **149**, 223 (1994).
11. F. Baletto, R. Ferrando, A. Fortunelli, F. Montalenti, C. Mottet, *J. Chem. Phys.* **116**, 3856 (2002).
12. Because the only degrees of freedom of the metal atoms in these clusters are vibrations, the entropic contributions to the free energy are small and differ very little with cluster size. Thus, Eq. 1 is also often applied to describe the size dependence of internal energy as well as free energy. Generally, γ is assumed to be independent of particle radius at the value for bulk metal (*3*, *4*, *13–15*).
13. X. Lai, D. W. Goodman, *J. Mol. Catal.* **A162**, 33 (2000).
14. M. J. Jak *et al.*, *Surface Sci.* **474**, 28 (2001).
15. M. J. Jak, C. Konstapel, A. v. Kreuningen, J. Verhoeven, J. W. Frenken, *Surf. Sci.* **457**, 259 (2000).
16. D. E. Starr, D. J. Bald, J. E. Musgrove, J. T. Ranney, C. T. Campbell, *J. Chem. Phys.* **114**, 3752 (2001).
17. The assumption of a constant number density of islands is probably slightly incorrect in that their number generally increases weakly with coverage in this range for such systems (*13*, *41*). Correcting for this would cause the measured decrease in stability with radius to be even more dramatic than shown.
18. W. R. Tyson, W. A. Miller, *Surf. Sci.* **62**, 267 (1977).
19. Using a very new value of γ for Pb [44 μJ/cm^2 (*42*)] gives even poorer agreement with experiment. Using Eq. 1 here neglects the energy of the flat face of the hemisphere, which is equivalent to setting the Pb/MgO adhesion energy at this face equal to the Pb-Pb adhesion energy. [If the Pb/MgO adhesion energy were zero, the factor of 2 in Eq. 1 would instead be 3. In reality, the needed correction is much smaller (*16*).]
20. I. Galanakis, N. Papanikolaou, P. H. Dederichs, *Surf. Sci.* **511**, 1 (2002).
21. R. C. Tolman, *J. Chem. Phys.* **17**, 333 (1949).
22. H. Z. Zhang, R. L. Penn, R. J. Hamers, J. F. Banfield, *J. Phys. Chem. B* **103**, 4656 (1999).
23. D. R. Lide, Ed., *CRC Handbook of Chemistry and Physics* (CRC Press, Boston, MA, ed. 77, 1996).
24. M. Methfessel, D. Hennig, M. Scheffler, *Appl. Phys.* **A55**, 442 (1992).
25. DePristo estimated that relation empirically by extrapolating between measured energies of: the gaseous dimer (CN = 1), a (111) surface (CN = 9), and the bulk (CN = 12). Furthermore, we used DePristo's relation to estimate the errors in the MBA model of Fig. 1 and found that the errors due to the decrease in bond energy with CN nearly compensate for the errors associated with extrapolating between only the most stable clusters, further justifying its use.
26. G. B. McVicker, R. L. Garten, R. T. Baker, *J. Catal.* **54**, 129 (1978).
27. We simplified the definition of E_{tot} ($= \Delta H_{sub} - E_{ad}^{support} + E_{diff}^{support}$) here slightly from that of W-J in that we neglected any excess activation energy (beyond the uphill reaction energy) associated with a monomer detaching from a metal particle to move onto the support surface, because this is tiny relative to E_{tot}.
28. There is another large error in Eq. 3. In its derivation, W-J expanded the exponential factors such as $e^{[\mu(R) - \mu(\infty)]/kT}$ in Taylor series and neglected all but the first two terms. This is equivalent to assuming that $\mu(R) - \mu(\infty)$ is small compared to kT. Inspection of the heat data in Fig. 1 proves that this is clearly not the case below 1000 K for particles with a radius of a few nanometers.
29. D. E. Starr, C. T. Campbell, *J. Phys. Chem.* **B105**, 3776 (2001).
30. C. E. Stassinos, H. H. Lee, *Chem. Eng. Sci.* **50**, 1337 (1995).
31. C. H. Bartholomew, Ed., *Sintering Kinetics of Supported Metals: Perspectives from a Generalized Power Law Approach*, vol. 88 of *Studies in Surface Science and Catalysis* (Elsevier Science, Amsterdam, Netherlands, 1994).
32. V. Bondzie, S. C. Parker, C. T. Campbell, *Catal. Lett.* **63**, 143 (1999).
33. F. Cosandey, T. E. Madey, *Surf. Rev. Lett.* **8**, 73 (2001).
34. S. C. Parker, A. W. Grant, V. A. Bondzie, C. T. Campbell, *Surf. Sci.* **441**, 10 (1999).
35. H. Graoui, S. Giorgio, C. R. Henry, *Philos. Mag. B* **81**, 1649 (2001).
36. C. T. Campbell, D. E. Starr, *J. Am. Chem. Soc.* **124**, 9212 (2002).
37. The average initial radius of Au clusters grown on TiO_2(110) under similar deposition conditions was estimated by scanning tunneling microscopy (*13*) and high-resolution scanning electron microscopy (*33*) to be about 1 nm. We used a slightly smaller average size because those techniques could have missed the smallest particles.
38. M. Gillet, A. A. Mohammed, K. Masek, E. Gillet, *Thin Solid Films* **374**, 134 (2000).
39. S. C. Parker, thesis, University of Washington, Seattle, WA (2000).
40. S. H. Overbury, P. A. Bertrand, G. A. Somorjai, *Chem. Rev.* **75**, 547 (1975).
41. C. R. Henry, M. Meunier, *Mat. Sci. Eng.* **A217/218**, 239 (1996).
42. C. Bombis, A. Emundts, M. Nowicki, H. P. Bonzel, *Surf. Sci.* **511**, 83 (2002).

43. We thank the U.S. Department of Energy, Office of Basic Energy Sciences, Chemical Sciences Division, for support of this work. D.E.S. thanks NSF and the University of Washington Center for Nanotechnology for an IGERT Fellowship.

14 June 2002; accepted 24 September 2002

Heterogeneous Atmospheric Aerosol Production by Acid-Catalyzed Particle-Phase Reactions

Myoseon Jang,* Nadine M. Czoschke, Sangdon Lee, Richard M. Kamens

According to evidence from our laboratory, acidic surfaces on atmospheric aerosols lead to potentially multifold increases in secondary organic aerosol (SOA) mass. Experimental observations using a multichannel flow reactor, Teflon (polytetrafluoroethylene) film bag batch reactors, and outdoor Teflon-film smog chambers strongly confirm that inorganic acids, such as sulfuric acid, catalyze particle-phase heterogeneous reactions of atmospheric organic carbonyl species. The net result is a large increase in SOA mass and stabilized organic layers as particles age. If acid-catalyzed heterogeneous reactions of SOA products are included in current models, the predicted SOA formation will be much greater and could have a much larger impact on climate forcing effects than we now predict.

Gas-phase reactions of volatile organic compounds (VOCs) associated with photochemical oxidant cycles have been of great interest in predicting ozone (O_3) concentrations and, more recently, SOA formation. SOA has received much attention for a variety of reasons, many of which are associated with the establishment of a national ambient air quality standard for atmospheric fine particles (*1*). From a public health perspective, SOAs, which are a major contributor to fine particulate matter, have potentially negative health effects. In particular, it is now believed that the potency of a mixture of environmental chemicals, such as an organic and inorganic multicomponent SOA, may be greater than its constitutive parts (*1*). At the regional scale, SOA formation can contribute to the formation of visibility-reducing haze (*2*). SOAs affect the Earth's radiative balance (*3*, *4*) directly by altering the scattering properties of the atmosphere and indirectly by changing cloud properties. These climate forcing effects are thought to lead to a net cooling effect at the tropospheric level (*3*). Furthermore, the composition of SOAs influences the extent of these effects. For example, the water content of cloud aerosols, and thus a cloud's lifetime, is mainly influenced by particle acidity and sulfate content.

Our understanding of the role SOAs play in climate change and their connection to health effects is limited by numerous uncertainties, particularly the total SOA particle concentration and mass, the contribution of tropospheric SOAs to the total particle load, the composition and physical structure of atmospheric aerosols, and the heterogeneous chemistry that influences these parameters. What is known is that biogenic terpenes from terrestrial vegetation (*5*) and aromatics from anthropogenic sources (*6*) are SOA precursors. Also, the gas-phase photooxidation reaction of these VOCs generates large amounts of multifunctional organic carbonyls (*7–10*), which are major SOA components. In addition, these components may react heterogeneously to form an additional generation of products in the particle phase.

A major class of these heterogeneous reactions is the acid-catalyzed reactions of atmospheric carbonyls (*10*, *11*). Principal candidates for atmospheric acid catalysts are sulfuric acid (H_2SO_4) and nitric acid (HNO_3), which are produced through oxidation processing of SO_2 and NO_x emitted from fossil fuel combustion (*12–15*). These are inorganic acids; thus, the effects of acid-catalyzed heterogeneous reactions are essentially interac-

Department of Environmental Sciences and Engineering, CB 7431, Rosenau Hall, University of North Carolina at Chapel Hill, Chapel Hill, NC 27599, USA.

*To whom correspondence should be addressed. E-mail: mjang@email.unc.edu

tions between the organic and inorganic portions of aerosols. Unfortunately, most work focusing on inorganic aerosols neglects the organic aerosol fraction. Similarly, studies of SOA formation tend to be conducted without considering inorganic components.

The accommodation properties of organic species in the aerosol phase, and thus SOA mass, have been addressed primarily by condensation or thermodynamic gas-particle partitioning (*8*, *16*, *17*). However, these theories currently do not account for heterogeneous reactions, such as the acid-catalyzed carbonyl chemistry that takes place in the particle phase (*11*). Such chemistry includes diverse acid-catalyzed reactions such as hydration, polymerization, hemiacetal and acetal formation, aldol condensation, ring opening of terpenoid carbonyls, and cross-linking in the aerosol media (Fig. 1). The key players in these reactions are atmospheric carbonyls, the water content of aerosols, inorganic acids, and possibly alcohols. For example, it is known that the equilibrium between an aldehyde and its hydrate is quickly established and often favors the hydrate form (*18*). Carbonyls may further react with the hydroxy groups of hydrates, resulting in higher molecular weight dimers, trimers, and polymers (*11*, *18*). Hemiacetal formation is often unstable, and they exist only in equilibrium. However, Tobias and Ziemann (*19*) have shown the formation of large peroxyhemiacetals from the reaction of an α-acyloxyalkyl hydroperoxide with formaldehyde. In the presence of acids, further reaction of hemiacetals leads to acetals, which are much more stable (*20*).

Sources of the atmospheric acids, HNO_3 and H_2SO_4, are ultimately associated with the burning of fossil fuels. For example, diesel combustion produces SO_2, which results in acidic soot particles (*13*, *14*). It is presently known that H_2SO_4 makes up 1.2 to 5.3% of the mass of the small (mass median diameter ≈ 40 nm) diesel particles at 40% engine load (*13*). The current average sulfur content of diesel fuels in the United States is capped at 500 ppm; however, further reductions to 15 ppm are being considered as early as 2006. These acids are also scavenged with ammonia, forming ammonium sulfate and ammonium nitrate (*21*). Although ammonia can reduce acidity in the atmospheric environment, the long-range transportation of ammonia can actually result in acidification and eutrophication by enriching soils and aqueous environments with nitrogen (*22*).

Although the constituents and conditions for acid-catalyzed heterogeneous reactions have always been present, their products often fail to be identified due to sampling and analysis procedures (such as solvent extractions and derivitization procedures) in which hemiacetals, acetals, hydrates, and polymeric structures can easily return to their original aldehydes (*20*). This reversion renders these products undetected but leads to positive artifacts of their parent carbonyls and alcohols.

The organic aerosol yields of different aliphatic aldehydes in the presence or absence of an acid catalyst (H_2SO_4) as observed in 0.5-m^3 Teflon-film bags are shown in Fig. 2A. There is a marked increase in organic aerosol yield in an acidic environment due to heterogeneous reactions. Our results suggest that acid-catalyzed heterogeneous reactions of aliphatic aldehydes can increase organic aerosol formation by as much as a factor of 5 when compared to neutral aerosol systems. Such reactions could be of particular importance in natural systems because of the large emissions of aldehydes from vegetation, including aliphatic (carbon numbers 6 to 10) aldehydes (*11*), trans-2-hexenal (*23*, *24*), and a host of similar aldehydes.

Also shown in Fig. 2A are the yields for glyoxal, which are perhaps even more interesting. The extremely high volatility of glyoxal (boiling point, 50.4°C) suggests that it would be an unlikely contributor to aerosol mass. Yet, its α-dicarbonyl functionality makes it very reactive toward heterogeneous reactions and results in relatively high aerosol yields. In addition, glyoxal or similar α-bicarbonyls (e.g., methylglyoxal and 3-hydroxy-2-oxo-propanal), tricarbonyls (e.g., trioxopropane and 2,3-dioxobutanal), and multifunctional conjugated carbonyls are products of atmospheric oxidations of aromatics (*10*) or biogenic hydrocarbons, such as iso-

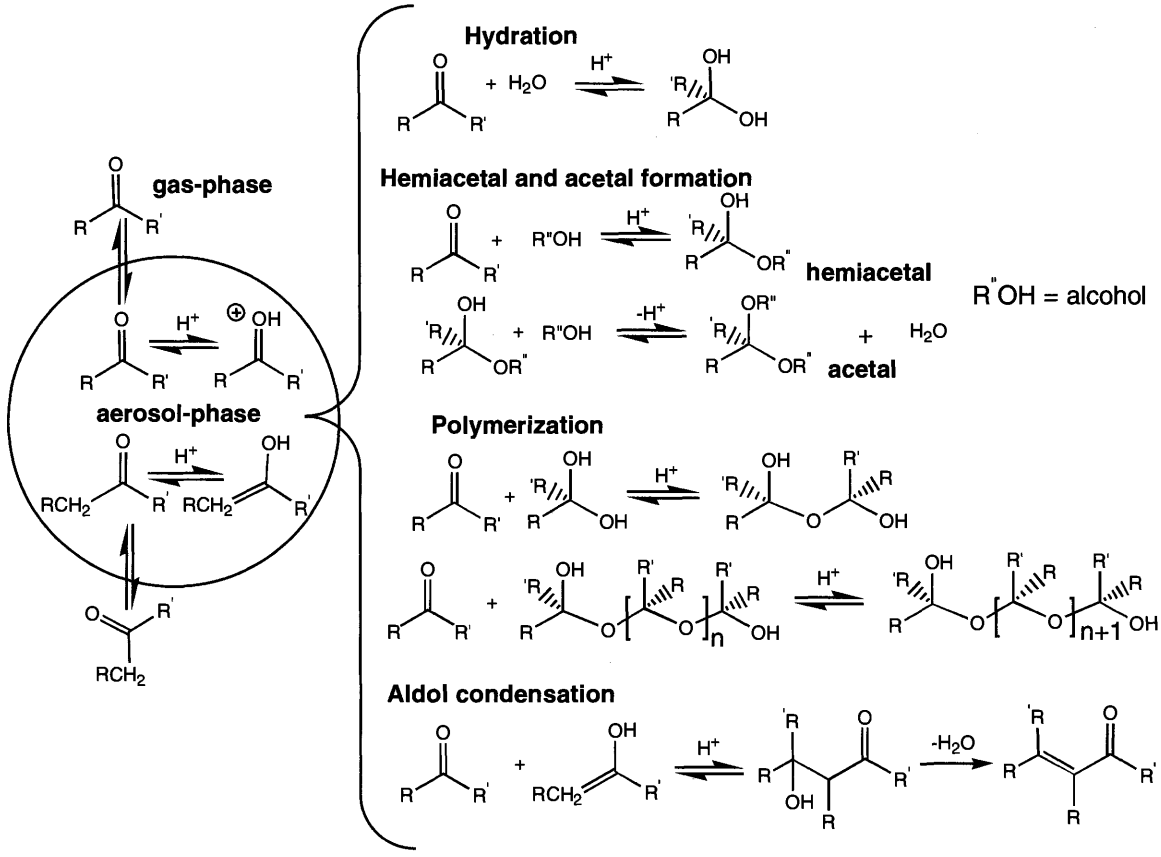

Fig. 1. Acid-catalyzed heterogeneous reaction mechanisms of atmospheric carbonyls.

prene (*25*). All of these compounds are expected to increase SOA mass through acid-catalyzed heterogeneous reactions.

The amplified SOA yields as a result of heterogeneous reaction of the above-mentioned products are illustrated in Fig. 2B. The simplest of the biogenic VOCs, isoprene and acrolein, were reacted in 0.5-m^3 Teflon bags containing O_3 and either acidic or nonacidic inorganic seed aerosols. The SOA yields, normalized by O_3 concentration and seed volume, are larger in the acidic systems. Conjugated carbonyls such as methacrolein and methylvinylketones are major products of the isoprene-O_3 reaction, and further oxidation of these products leads to α-dicarbonyls.

Another indication of heterogeneous reactions is positive deviation from expected gas-particle partitioning. The partitioning coefficient, K_p, of a compound is determined experimentally as the ratio of particle-phase concentration (ng μg^{-1}) to gas-phase concentration (ng m^{-3}) and can be predicted thermodynamically from its activity coefficient and vapor pressure, P_L^0 (*10*, *26*, *27*). As mentioned, many carbonyl products of heterogeneous reactions revert back to their parent compounds during analysis and cause positive artifacts of these carbonyl compounds (*8*, *10*). We compared the K_p values for the major aerosol-phase carbonyl products of the photooxidation of toluene (one of the most prevalent aromatic VOCs) in the presence of NO_x from experiments in a 190-m^3 outdoor smog chamber (table S1). The K_p of carbonyl products shows exceedingly positive deviations, but those of phenolic and quinonoid products, such as 2-methyl-4-nitrophenol and 2-methylquinone, tend to agree with partitioning theory (*10*). The relatively "high" vapor pressures of carbonyl products also indicate that they should not partition appreciably to the particle phase, yet they are observed. In an extreme example, the partitioning of 2-hydroxy-1,3-propanedial in table S1 is three orders of magnitude higher than its predicted K_p (*10*) because of heterogeneous reactions.

Similar behavior is observed for other SOA products from the photooxidation of biogenic terpenes. We also estimated the K_p values for *cis*-pinonaldehyde, a major carbonyl product of the photooxidation of α-pinene, in the presence of NO_x (table S1). The experimental K_p of *cis*-pinonic acid (a major carboxylic acid product) agrees with equilibrium partitioning predictions, but that of *cis*-pinonaldehyde on diesel soot shows a large deviation. Diesel soot, because of its H_2SO_4 content, can initiate acid-catalyzed heterogeneous reactions. Compared to fossil fuels, biomass combustion is a minor source of SO_2 (*28*). Yet wood soot also resulted in a measurable positive deviation from theoretical partitioning compared to the photooxidation reaction system of α-pinene and NO_x without background aerosol (table S1). Thus, even small amounts of acid are capable of catalyzing heterogeneous reactions.

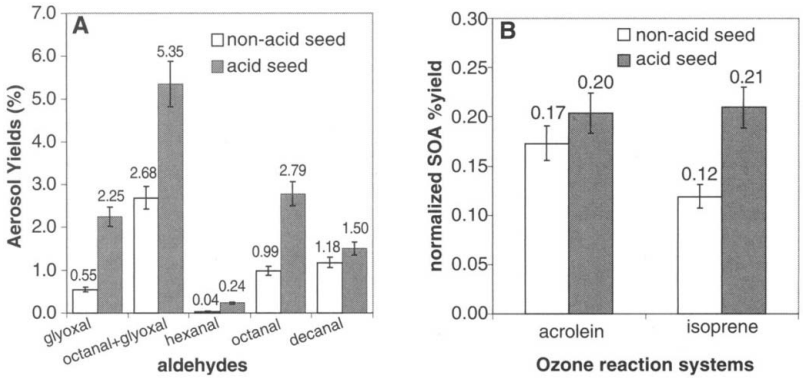

Fig. 2. (**A**) Organic aerosol yields from heterogeneous reactions of aldehydes and 1-decanol with and without an acid catalyst. The aerosol yields were calculated by dividing the organic aerosol mass by the mass of the injected liquid organic in the bag air phase (*32*). (**B**) SOA yields from the O_3 reaction systems of acrolein and isoprene in the presence and absence of an acid catalyst. The SOA yields were normalized by O_3 and initial VOC concentrations (*33*).

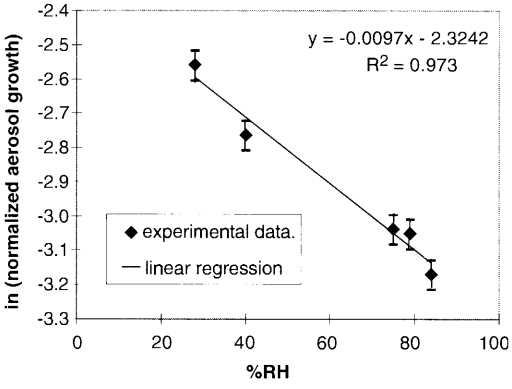

Fig. 3. The relationship between %RH and aerosol growth (normalized by the seed aerosol volume and the gas-phase octanal concentration) in the presence of an acid catalyst.

Heterogeneous reactions may be strongly influenced by environmental conditions. The reactions are likely most influenced by the relationship between particle acidity and relative humidity (%RH) (*29*). Observations of aerosol growth from heterogeneous reactions of octanal on acidic and nonacidic seed aerosol at varying %RH in a flow reactor corroborate this relationship. As shown in Fig. 3 (*29*, *30*), there is a strong linear relationship (r^2 = 0.97) between %RH and the log of aerosol growth (normalized for the volume of inorganic seed and the gas-phase concentration of octanal) when an acid catalyst is present. In the absence of an acid catalyst, aerosol growth is neither sensitive to nor linear with %RH.

A final method of observing heterogeneous reactions is through detection of functional group transformation by Fourier transform infrared spectroscopy (FTIR). Organic aerosols have been collected on ungreased ZnSe disks by impaction for FTIR analysis (*10*, *11*, *31*). Unfortunately, organic aerosols generated without an acid catalyst were too small or too volatile to have a collection efficiency that was high enough for measurement. Thus, spectra of aerosols from acid and nonacid systems cannot be compared. However, the difficulty in collecting nonacid aerosols is in itself an indication that they differ fundamentally from those formed in an acidic environment. Figure 4 illustrates typical FTIR spectra of organic aerosols formed by acid-catalyzed heterogeneous reactions of glyoxal and the products from the reaction of O_3 with isoprene or acrolein. All three acid-catalyzed systems exhibited the O–H stretch at 3100 to 3600 cm^{-1}. In particular, the FTIR bands at 1180 (C–O–C stretch of hemiacetals and acetals), 1052 (C–C–O asymmetric stretch of alcohols), 882 (C–C–O symmetric stretch of alcohols), and 584 cm^{-1} (-OH out of plane) strongly confirm the functional group transformation of carbonyl species with an acid catalyst. Equally telling is that the carbonyl stretch (1640 to 1780 cm^{-1}) in all systems was very weak, indicating that the carbonyl had been transformed.

A rather interesting attribute of the FTIR spectra of the O_3 reaction products of isoprene and acrolein (Fig. 4) is that they all have absorption peaks similar to those of glyoxal aerosols in the presence of an acid catalyst. These similarities are evidence that dicarbonyl products of isoprene and acrolein oxidation react heterogeneously to form polymeric structures or hydrates in the particle phase. Additionally, the FTIR

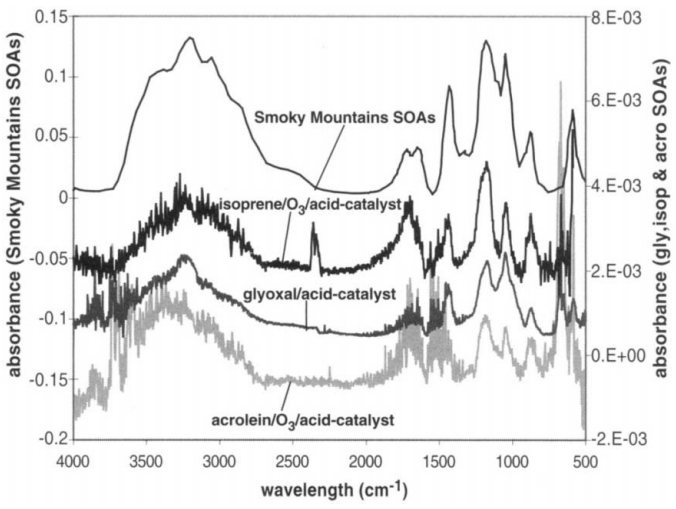

Fig. 4. FTIR spectra of organic aerosols impacted on an ungreased ZnSe FTIR disk for the glyoxal–$(NH_4)_2SO_4$-H_2SO_4 system and SOAs from the reaction of O_3 with isoprene and acrolein in the presence of an acid catalyst (H_2SO_4). The FTIR spectrum for SOAs from the Smoky Mountains was obtained from Blando *et al.* (*31*): FTIR spectrum of 0.5- to 1.0-μm aerosols collected on 13 August 1995 at Look Rock, Smoky Mountains, Tennessee. Axis label E–03 indicates $\times 10^{-3}$.

spectra from size-resolved particle samples collected from the Southeastern Aerosol Visibility Study in the Smoky Mountains at Look Rock by Blando *et al.* (*31*) also show similar peaks at 589, 878, 1049, and 1182 cm^{-1}. This spectrum suggests that the organics comprising SOAs from the Smoky Mountains natural aerosol also have functional group transformations similar to those in our laboratory isoprene and acrolein aerosols. We believe that these transformations are due to acid-catalyzed heterogeneous reactions, which are therefore a major contributor to SOA formation in natural systems.

Our results strongly suggest that inorganic acids, such as H_2SO_4, catalyze carbonyl heterogeneous reactions and consequently lead to a large increase in SOA production. Thus, both inorganic and organic constituents need to be considered for an accurate explanation of SOA formation. For example, we believe that scenarios for high SOA formation and high concentrations of atmospheric inorganic acids may be coincident. Additionally, biogenic and anthropogenic emissions of carbonyl species associated with photooxidation cycles are considerable. Processing these carbonyl compounds via particle-phase heterogeneous reactions constitutes a previously unstudied, and to date unquantified, source of global aerosol material. The importance of quantifying global aerosol mass is key to understanding the climate forcing properties of aerosols. Thus, the role of heterogeneous reactions in SOA formation needs to be considered in climate change prediction models.

References and Notes

1. "Air quality criteria for particulate matter" [EPA/600/P-95/001cF, Environmental Protection Agency (EPA), Washington, DC, 1996].
2. R. L. Tanner, W. Parkhurst, *J. Air Waste Manage. Assoc.* **50**, 1299 (2000).
3. J. E. Hansen, M. Sato, *Proc. Natl. Acad. Sci. U.S.A.* **98**, 14778 (2001).
4. J. M. Adams, J. V. H. Constable, A. B. Guenther, P. Zimmerman, *Chemosphere-Global Change Sci.* **3**, 73 (2001).
5. A. P. Altshuller, *Atmos. Environ.* **17**, 2131 (1983).
6. H. E. Jeffries, in *Composition, Chemistry, and Climate of the Atmosphere*, H. B. Singh, Ed. (Van Nostrand Reinhold, New York, 1995), pp 308–348.
7. B. Noziere, I. Barnes, K. H. Becker, *J. Geophys. Res.* **104**, 23645 (1999).
8. R. M. Kamens, M. Jang, C. J. Chien, K. Leach, *Environ. Sci. Technol.* **33**, 1430 (1999).
9. J. Yu, H. E. Jeffries, K. G. Sexton, *Atmos. Environ.* **31**, 2261 (1997).
10. M. Jang, R. M. Kamens, *Environ. Sci. Technol.* **35**, 3626 (2001).
11. ———, *Environ. Sci. Technol.* **35**, 4758 (2001).
12. B. J. Finlayson-Pitts, J. N. Pitts, *Chemistry of the Upper and Lower Atmosphere: Theory, Experiments, and Applications* (Academic Press, New York, 2000), pp. 207–213.
13. H. J. Tobias *et al.*, *Environ. Sci. Technol.* **35**, 2233 (2001).
14. M. S. Reddy, C. Venkataraman, *Atmos. Environ.* **36**, 677 (2002).
15. J. Curtius *et al.*, *J. Geophys. Res.* **106**, 31975 (2001).
16. J. R. Odum, T. P. W. Jungkamp, J. H. Seinfeld, *Science* **276**, 96 (1997).
17. T. Hoffmann *et al.*, *J. Atmos. Chem.* **26**, 189 (1997).
18. D. Barton, in *Comprehensive Organic Chemistry: The Synthesis and Reactions of Organic Compounds*, W. D. Ollis, Ed. (Pergamon Press, New York, 1979), pp. 960–1013.
19. H. J. Tobias, K. S. Docherty, D. E. Beving, P. J. Ziemann, *Environ. Sci. Technol.* **34**, 2116 (2000).
20. F. A. Carey, R. J. Sundberg, *Advanced Organic Chemistry: Part A Structure and Mechanisms* (Plenum Press, New York, ed. 4, 2000).
21. M. T. Nguyen, A. Jamka, R. Cazar, F. M. Tao, *J. Chem. Phys.* **106**, 8710 (1997).
22. H. W. Paerl, *Environ. Sci. Technol.* **36**, 323A (2002).
23. J. Kesselmeier, M. Staudt, *J. Atmos. Chem.* **33**, 23 (1999).
24. A. M. Winer *et al.*, *Atmos. Environ.* **26A**, 2647 (1992).
25. R. M. Kamens *et al.*, *Int. J. Chem. Kinet.* **14**, 955 (1982).
26. M. Jang, R. M. Kamens, K. Leach, M. R. Strommen, *Environ. Sci. Technol.* **31**, 2805 (1997).
27. J. F. Pankow, *Atmos. Environ.* **28**, 2275 (1994).
28. M. S. Reddy, C. Venkataraman, *Atmos. Environ.* **36**, 699 (2002).
29. M. Jang, S. Lee, R. M. Kamens, in preparation.

30. Gas-phase octanal was introduced with an air stream to the main body of the glass flow reactor (2.2-m length × 2.5-cm inner diameter). The aerosol population sampled at ports spaced sequentially down the flow reactor was observed in the presence of an acid catalyst with a scanning mobility particle sizer. The %RH was varied by controlling the water-saturator. The experimental temperature was 295 to 296 K.
31. J. D. Blando *et al.*, *Environ. Sci. Technol.* **32**, 604 (1998).
32. Before the addition of hydrocarbons, seed aerosols were injected to the Teflon bags by nebulizing aqueous salt solution: 0.0067 M of $(NH_4)_2SO_4$ solution for nonacid seed and 0.005 M H_2SO_4 plus 0.0035 M of $(NH_4)_2SO_4$ for acid seed. Also note that the organic loss by the reaction on the wall surface will be higher as the molecular weight of aliphatic aldehydes increases.
33. The normalized aerosol yield for isoprene-O_3 was averaged from the data on 20 February 2001 and 24 February 2001. Two different sets of experiments on 24 February 2001 were used for the acrolein-O_3 systems. The initial O_3 concentration was 0.57 ppm. The experimental temperature was 295 to 296 K and %RH was 45 to 50%.

34. Supported by a grant from NSF (grant ATM 9708533) and a Science To Achieve Results grant from EPA (grant R-82817601-0) to the University of North Carolina at Chapel Hill.

Supporting Online Material

www.sciencemag.org/cgi/content/full/298/5594/814/DC1
Table S1

5 July 2002; accepted 20 September 2002

Robotic Observations of Dust Storm Enhancement of Carbon Biomass in the North Pacific

James K. B. Bishop,[1]* Russ E. Davis,[2] Jeffrey T. Sherman[2]

Two autonomous robotic profiling floats deployed in the subarctic North Pacific on 10 April 2001 provided direct records of carbon biomass variability from surface to 1000 meters below surface at daily and diurnal time scales. Eight months of real-time data documented the marine biological response to natural events, including hydrographic changes, multiple storms, and the April 2001 dust event. High-frequency observations of upper ocean particulate organic carbon variability show a near doubling of biomass in the mixed layer over a 2-week period after the passage of a cloud of Gobi desert dust. The temporal evolution of particulate organic carbon enhancement and an increase in chlorophyll use efficiency after the dust storm suggest a biotic response to a natural iron fertilization by the dust.

Marine phytoplankton biomass is replaced, on average, once every 1 to 2 weeks (*1*–*3*). Carbon products of photosynthesis (*4*), i.e., particulate organic carbon (POC), particulate inorganic carbon (PIC), and dissolved organic carbon (DOC), are exported below 100 m at a rate of